





Hypoxia-induced ELF3 promotes tumor angiogenesis through IGF1/IGF1R

Seung Hee Seo¹ , Soo-Yeon Hwang¹ , Seohui Hwang¹, Sunjung Han¹, Hyojin Park¹, Yun-Sil Lee¹ ,
Seung Bae Rho² & Youngjoo Kwon^{1,*} 

Abstract

Epithelial ovarian cancer (EOC) is one of the most lethal gynecological cancers despite a relatively low incidence. Angiogenesis, one of the hallmarks of cancer, is essential for the pathogenesis of EOC, which is related to the induction of angiogenic factors. We found that ELF3 was highly expressed in EOCs under hypoxia and functioned as a transcription factor for IGF1. The ELF3-mediated increase in the secretion of IGF1 and VEGF promoted endothelial cell proliferation, migration, and EOC angiogenesis. Although this situation was much exaggerated under hypoxia, ELF3 silencing under hypoxia significantly attenuated angiogenic activity in endothelial cells by reducing the expression and secretion of IGF1 and VEGF. ELF3 silencing attenuated angiogenesis and tumorigenesis in *ex vivo* and xenograft mouse models. Consequently, ELF3 plays an important role in the induction of angiogenesis and tumorigenesis in EOC as a transcription factor of IGF1. A detailed understanding of the biological mechanism of ELF3 may both improve current antiangiogenic therapies and have anticancer effects for EOC.

Keywords ELF3; hypoxia; insulin-like growth factor I; ovarian cancer; tumor angiogenesis

Subject Categories Cancer; Signal Transduction; Vascular Biology & Angiogenesis

DOI 10.15252/embr.202152977 | Received 30 March 2021 | Revised 9 May 2022 | Accepted 19 May 2022 | Published online 13 June 2022

EMBO Reports (2022) 23: e52977

Introduction

Angiogenesis is closely involved in both normal ovarian physiology (Robinson *et al.*, 2009), and the progression and metastasis of ovarian cancer (OC) (Spannuth *et al.*, 2008; Graybill *et al.*, 2015). Epithelial ovarian cancer (EOC) accounts for more than 90% of OCs. Most EOC patients are diagnosed at advanced stages (III/IV) because the early stages are usually asymptomatic. Patients typically have a poor prognosis due to extensive metastasis to the omentum, liver, and lungs (Coleman *et al.*, 2013; Burger *et al.*, 2014). Epithelial ovarian cancer is initially sensitive to platinum-based therapies, but

most patients eventually experience relapse and gradually become resistant to platinum drugs (Cannistra, 2004). Thus, targeted antiangiogenic therapy has been introduced to treat recurrent, platinum-resistant EOC. Antiangiogenic drugs, such as bevacizumab, pazopanib, aflibercept, and ramucirumab, inhibit angiogenic factors that are excessively secreted from tumors, receptors, or kinases involved in the angiogenesis of vascular endothelial cells. These drugs block the nutrient supply to cancer cells and block tumor metastasis. Bevacizumab was initially approved by the U.S. Food and Drug Administration (FDA) in 2004 for metastatic colorectal cancer and was approved for advanced OC patients in 2018. Of the various antiangiogenic drugs, bevacizumab has been most widely studied in various tumor types, particularly in EOC, and has been reported to improve the progression-free survival (PFS) of EOC patients when combined with chemotherapy, such as carboplatin and paclitaxel (Wang *et al.*, 2018a). However, there are reports that bevacizumab does not have a direct effect on tumors, so it is less effective on already grown tumors, and it has limitations in long-term use due to serious side effects such as thrombosis (Kerbel & Folkman, 2002; Dey *et al.*, 2015). Therefore, understanding the biological mechanisms involved in angiogenesis in EOC is essential to develop effective antiangiogenic agents with different mechanisms from the existing drugs.

The angiogenic switch balances proangiogenic and antiangiogenic factors in normal tissues but not in cancer (Bergers & Benjamin, 2003). As cancer grows, the tumor microenvironment gradually becomes hypoxic. Under hypoxic conditions, the tumor promotes angiogenesis towards the surrounding blood vessels by hypersecreting proangiogenic factors, such as vascular endothelial growth factor (VEGF), insulin-like growth factors (IGF1), fibroblast growth factor-2, platelet-derived growth factor, the angiopoietins, hepatocyte growth factor, tumor necrosis factor, and interleukin-6 (Potente *et al.*, 2011; Ribatti *et al.*, 2012; Yadav *et al.*, 2015). Among various proangiogenic factors, IGF1 plays an essential role in biological processes such as the development, migration, and tube formation of endothelial cells (ECs). IGF1 promotes the stability of hypoxia-inducing factor-1 alpha (HIF-1 α) increasing its protein level, thereby enhancing VEGF expression (Fukuda *et al.*, 2002; Treins *et al.*, 2002; Stoeltzing *et al.*, 2003). IGF1 induces the epithelial to mesenchymal transition (EMT) by indirectly mediating the

¹ College of Pharmacy, Graduate School of Pharmaceutical Sciences, Ewha Womans University, Seoul, Korea

² Research Institute, National Cancer Center, Goyang-si Gyeonggi-do, Korea

*Corresponding author. Tel.: +82 232774653; fax: +82 232772851; E-mail: ykwon@ewha.ac.kr

activation of matrix metalloproteinases (MMPs) through PI3K and MAPK pathways (Walsh & Damjanovski, 2011). Moreover, IGF1 activates EC metabolism by enhancing glucose absorption (Boes et al, 1991).

Given that angiogenesis is activated by various complex events such as differentiation, proliferation, migration, metabolism, and cell-cell communication of ECs, we thought that various transcription factors (TFs) could be involved in the angiogenesis process (Jeong et al, 2017). Therefore, we sought to identify a TF that exhibits key functions specific to EOC among the TFs activated under the hypoxic tumor microenvironment. With an unbiased approach through analysis using a variety of bioinformatics tools, we found that an E74-like ETS transcription factor 3 (ELF3, also known as ESE-1 and ESX) was most highly expressed in EOC (Fig 1). ELF3 is a TF that acts bidirectionally as an oncogene or tumor suppressor gene depending on the type of cancer. ELF3 is epithelial-specific and is involved in a wide

range of biological processes such as cell proliferation, migration, EMT, and invasion of various epithelial tumors (Walker et al, 2010; Longoni et al, 2013; Wang et al, 2014, 2018b; Kar & Gutierrez-Hartmann, 2017; Kar et al, 2017; Zhao et al, 2018; Zheng et al, 2018; Chen et al, 2019; Gondkar et al, 2019; Li et al, 2019; Zhang et al, 2020, 2021). In recently published papers, ELF3 was considered to be a key biomarker to diagnose and predict ovarian serous cancer (Xu et al, 2021; Zhang et al, 2021). ELF3 overexpression is reported to promote the pathogenesis of OC through the mTOR signaling pathway and induce cisplatin resistance in OCs (Liu et al, 2021). Furthermore, ELF3 is also known to promote OC cell growth and metastasis by inhibiting miR-485-5p transcription, which interferes with the CLDN4/Wnt/ β -catenin axis (Kuang & Li, 2021). A number of researchers continue to investigate the relationship between OC and ELF3. Nevertheless, few studies have reported that ELF3 can possibly regulate angiogenesis in OC.

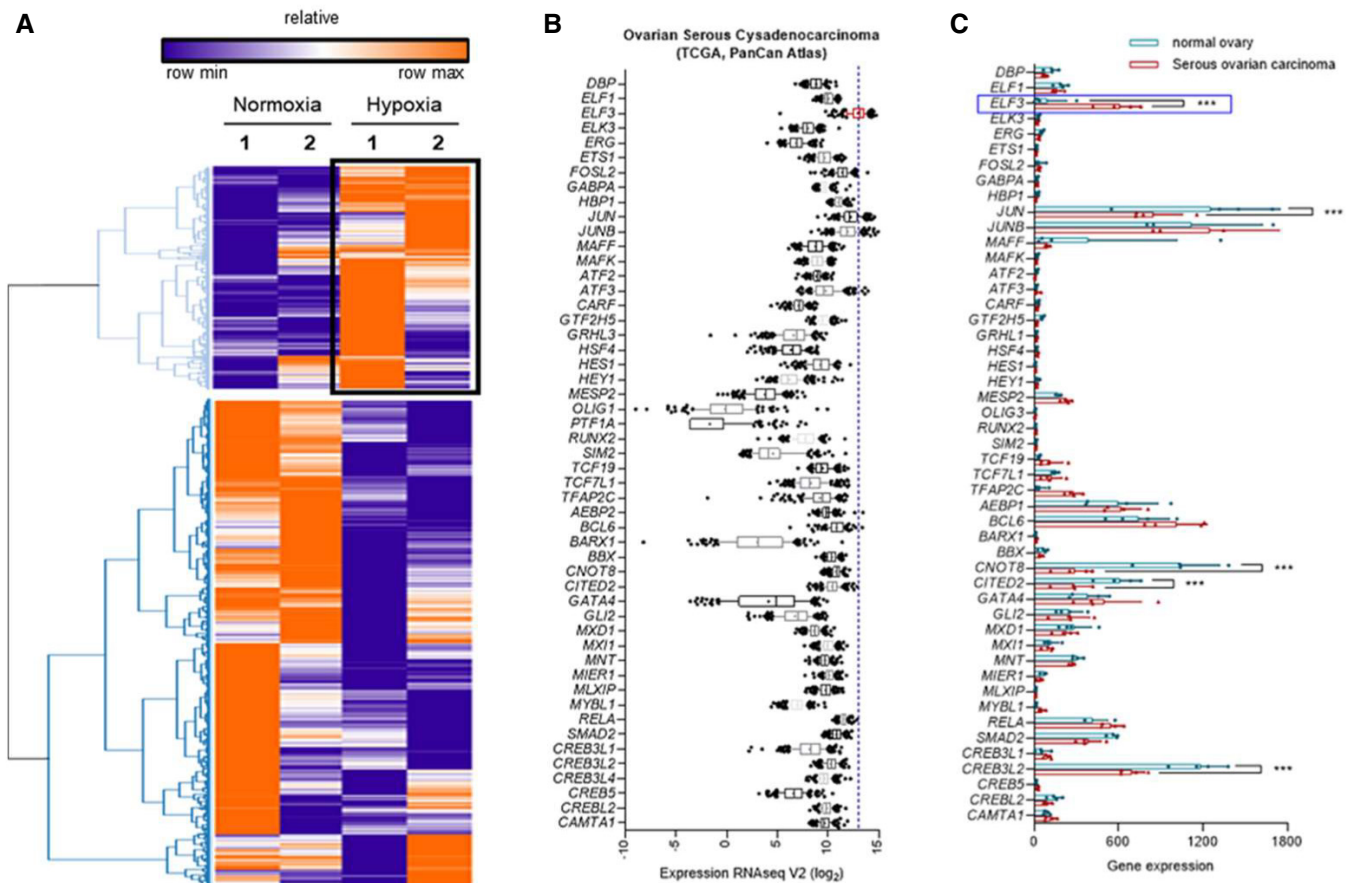


Figure 1. ELF3 expression was upregulated in ovarian cancer under hypoxic conditions.

- A** The heat map shows the relative expression of genes with a > 1.5-fold difference between normoxia and hypoxia in a human OC cell dataset (GSE55564). Genes highlighted in a black box are selected as overexpressed genes by hypoxia through hierarchical clustering based on a one minus Pearson correlation.
- B** Expression levels of selected 51 TFs were revalidated with the Pan-Cancer Atlas (PanCanAtlas) OC dataset ($n = 201$ patient samples). The vertical dashed line represents the mean of ELF3 expression, clearly showing that the mean of ELF3 expression is higher than the others.
- C** The difference in their expression was compared between normal ovaries and serous OCs (GSE36668) ($n = 4$ patient samples).

Data information: (B) The whiskers of the boxplot represent the 10–90th percentile and outliers are indicated by black dots. The “center line” and “+” in the boxplot represent the median and the mean, respectively. (C) Data are expressed as mean \pm SD. *** $P < 0.001$ vs. normal ovary (two-way ANOVA, Sidak’s).

In this study, we discovered and proved that ELF3 overexpression in OC induced tumor angiogenesis using several *in vitro*, *ex vivo*, and *in vivo* models. ELF3-mediated promotion of tumor angiogenesis occurred via transcriptional upregulation of IGF1 expression and secretion, thereby promoting endothelial proliferation, migration, and vascular sprouting. Comprehensively understanding the molecular mechanism of ELF3 as a key target to control tumor angiogenesis in OC may provide new insights for establishing effective therapeutic strategies to treat OC.

Results

ELF3 expression was upregulated in ovarian cancer under hypoxic conditions

Excessive growth of cancer cells increases oxygen consumption, and when the mass of the tumor exceeds the blood supply, the tumor microenvironment becomes hypoxic. Hypoxic stimulation causes the tumor to over-secrete proangiogenic factors and induce angiogenesis (Potente *et al*, 2011). Tumor angiogenesis, which is commonly found in OCs, has a great impact on oxygen and nutrient supply, and metastasis (Spannuth *et al*, 2008; Graybill *et al*, 2015). Therefore, we sought to identify TFs that are overexpressed in OCs under hypoxic conditions and are associated with angiogenesis. We compared gene expression differences between normoxia and hypoxia using GSE55564 (Koizume *et al*, 2015) and selected 13,477 genes showing more than 1.5-fold changes. To compare the expression of 13,477 genes, we performed hierarchical clustering (based on one minus Pearson correlation) and presented it in the form of a heat map (Fig 1A). 4,953 genes belonging to the same cluster and those overexpressed under hypoxic conditions were selected. Using the DAVID gene function classification tool, 51 TFs were selected among genes belonging to the transcription category (Table EV1). We then utilized the ovarian serous cystadenocarcinoma dataset from TCGA (PanCanAtlas, $n = 585$) and analyzed the gene expression levels of the 51 TFs selected from the prior step (cBioPortal v3.7.25; <https://www.cbioportal.org/>). Of all the TFs investigated, ELF3 was found to exhibit the highest expression in the OC dataset (Fig 1B). To confirm the significance of ELF3 in OC, we additionally investigated the expression level of the 51 TFs in both normal ovary and serous OC samples from the GSE36668 dataset (Elgaaen *et al*, 2012; Fig 1C). Here, ELF3 was identified as the gene showing the greatest expression difference between normal ovaries and OCs.

Collectively, as all data rationally implicates the significance of ELF3 overexpression on hypoxic OCs, we finally decided to focus on ELF3 to investigate its role in OC progression further.

ELF3 increased the expression of proangiogenic factors

First, we selected three EOC cell lines, SKOV3, Caov3, and OVCAR3, and investigated their protein and mRNA levels of ELF3 (Fig 2A and B). ELF3 was silenced in OVCAR3 in which ELF3 was highly expressed, and ELF3 was overexpressed in Caov3 with the lowest ELF3 expression level. Both ELF3 silencing and overexpression were induced in SKOV3. To investigate the relationship between the EOCs and angiogenesis, an angiogenic antibody array was performed to determine which targets of tumor angiogenesis are affected by ELF3 (Fig 2C). When ELF3 was overexpressed in SKOV3 cells, the protein level of IGF1 changed markedly, and MMPs and angiopoietin 1 (ANG1) slightly increased. Next, RT-qPCR and western blotting were performed in each type of EOC cell to confirm the array results. The mRNA and protein levels of proangiogenic factors, including IGF1, VEGF, ANG1, and MMP2, were increased in ELF3-overexpressed SKOV3 and Caov3 cells, and decreased in ELF3-silenced SKOV3 and OVCAR3 cells (Fig 2D and E).

ELF3 transcriptionally regulated IGF1 expression, thereby promoting the secretion of proangiogenic factors

Studies have shown that ELF3 transcriptionally regulates ANG1 (Brown *et al*, 2004). IGF1 has been shown to induce MMP activation and HIF-1 α stabilization through PI3K or MAPK signaling pathways (Fukuda *et al*, 2002; Treins *et al*, 2002; Stoeltzing *et al*, 2003; Walsh & Damjanovski, 2011; Fig EV1A). Therefore, we speculated that among the angiogenic factors increased in the array results, VEGF and MMP2 might be affected by ELF3-induced IGF1. To investigate this, changes in their expression were confirmed after silencing IGF1 in SKOV3 cells. When IGF1 was knocked down, ELF3 expression did not change, but the expression of VEGF and MMP2 was significantly reduced (Fig EV1B). In addition, despite the induction of ELF3 overexpression, IGF1 knockdown reduced the expression of VEGF and MMP2 again (Fig EV1C). To investigate the association between ELF3 and IGF1, we primarily analyzed public databases from TCGA and GEO, respectively. In the EOC patient database (TCGA, Firehose Legacy, $n = 200$) (cBioPortal v3.7.25 [<https://www.cbioportal.org/>]), ELF3 and IGF1 gene levels showed a positive correlation ($\gamma = 0.2076$, $P = 0.0032$) (Fig EV1D). In the

Figure 2. ELF3 in EOC cells increased the expression of proangiogenic factors involved in tumor angiogenesis.

- A, B ELF3 expression in EOC cell lines, SKOV3, OVCAR3, and Caov3, was characterized by (A) qPCR and (B) Western blot ($n = 3$ independent repetitions).
 C Membranes of an angiogenic antibody array were incubated with the lysates of SKOV3 cells transfected with empty vector (Ctrl) or ELF3. Antibodies targeting a total of 43 angiogenic factors were implanted on membranes 1 and 2 as indicated in the map format in the EV2 source data file. Proteins that change more than 1.5-fold compared with Ctrl are indicated by black boxes.
 D Representative images from the Western blotting analysis were performed in three independent experiments to verify the expression levels of proteins in ELF3- or siELF3-transfected EOC cells.
 E The mRNA levels of proangiogenic factors (*IGF1*, *VEGFA*, *MMPs*, and *ANGPT1*) were evaluated by RT-qPCR in ELF3- or siELF3-transfected EOC cells ($n = 5$ independent repetitions). The relative expression of each mRNA was normalized to β -actin and then calculated as fold change compared with the Ctrl or siCtrl groups, respectively.

Data information: Data are presented as mean \pm SD. (D) * $P < 0.05$, ** $P < 0.01$, *** $P < 0.001$ vs. Ctrl or siCtrl (two-way ANOVA, Sidak's). (E) * $P < 0.05$, ** $P < 0.01$, *** $P < 0.001$ vs. Ctrl (two-way ANOVA, Sidak's).

Source data are available online for this figure.

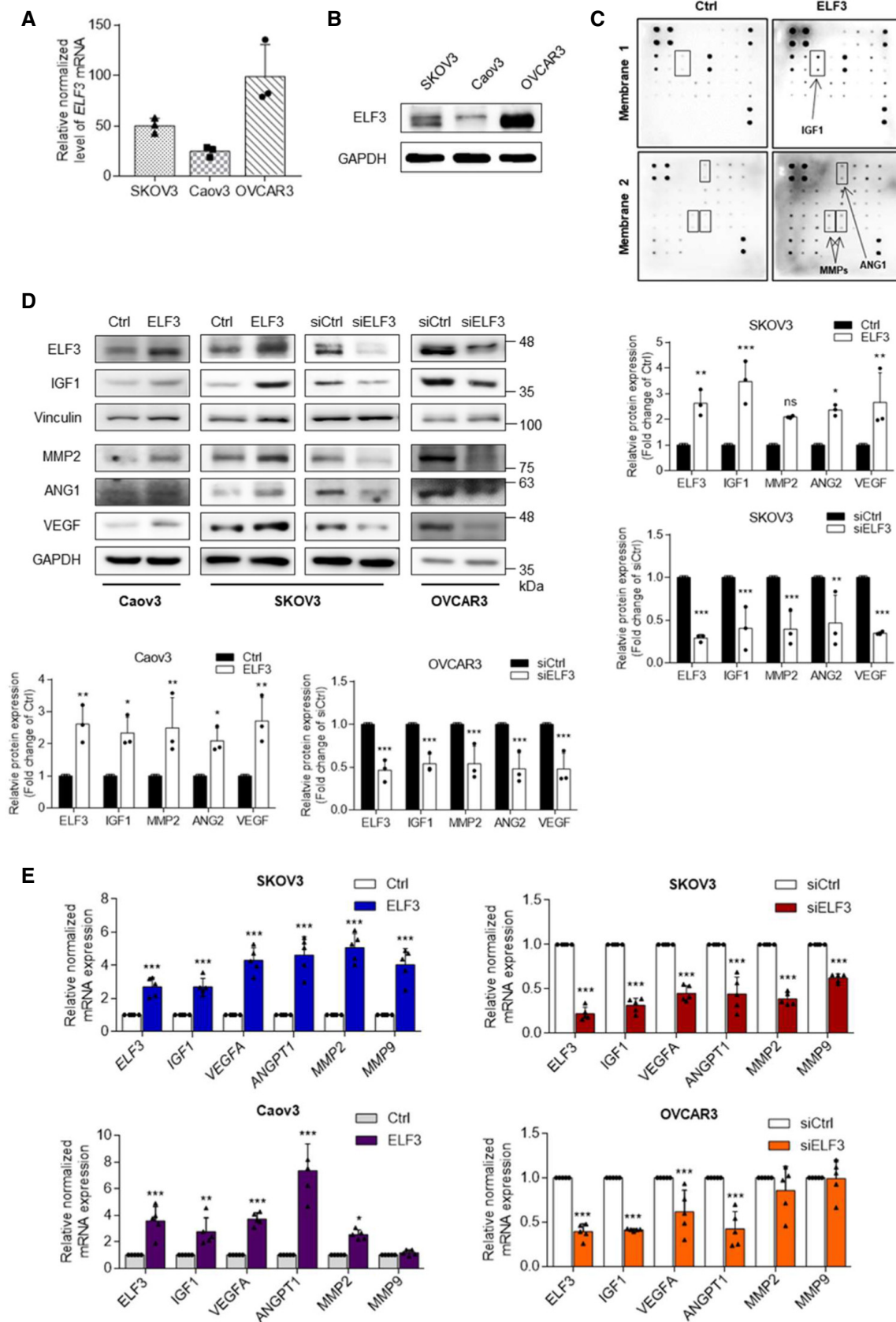


Figure 2.

GEO database (GSE36668), ELF3 expression showed an increasing pattern in the order of normal ovaries, borderline ovarian tumors, and ovarian carcinomas. IGF1 also showed a slightly increasing pattern, though this was not significant (Fig EV1E). As ELF3 and IGF1 expression obviously showed a positive correlation, we then checked whether ELF3 could function as a TF for IGF1. We predicted six ELF3 binding sites (ELF3-responsive elements, EREs) on the IGF1 gene promoter through eukaryotic promoter database (EPD) analysis (Fig 3A). Using the predicted EREs on the IGF1 promoter, chromatin immunoprecipitation (ChIP) and luciferase reporter gene assays were performed to demonstrate how ELF3 binds to the IGF1 promoter to regulate IGF1 expression. As a result of ChIP analysis using primers containing each predicted site (Fig 3A), when immunoprecipitation was performed with a negative control IgG, it was inferred that high expression of site3 was induced by nonspecific binding of IgG to site 3 (Fig 3B). However, upon immunoprecipitation with ELF3, the expression of site 4 was

specifically and significantly increased. Therefore, we found that ELF3 strongly binds to site 4 (−1,065 bp away from TSS) of the IGF1 promoter. After confirming that exogenous ELF3 binds to the full length of the IGF1 promoter (Fig 3C), we performed additional luciferase reporter gene assays using different IGF1 promoters in which six predicted binding sites were deleted one by one as shown in Fig 3D (left). Consistent with the results of the ChIP analysis, luciferase activity was lowest in the IGF1Δsite4 promoter (Fig 3D). Therefore, ELF3 upregulated IGF1 expression by binding to site 4 of the IGF1 promoter as a TF.

The ELF3/IGF1/IGF1R signaling axis accelerated tumor angiogenesis

In general, tumors stimulate ECs by hypersecreting proangiogenic factors to promote angiogenesis (Teleanu *et al*, 2019). Stimulated ECs promote angiogenic activities such as proliferation, migration,

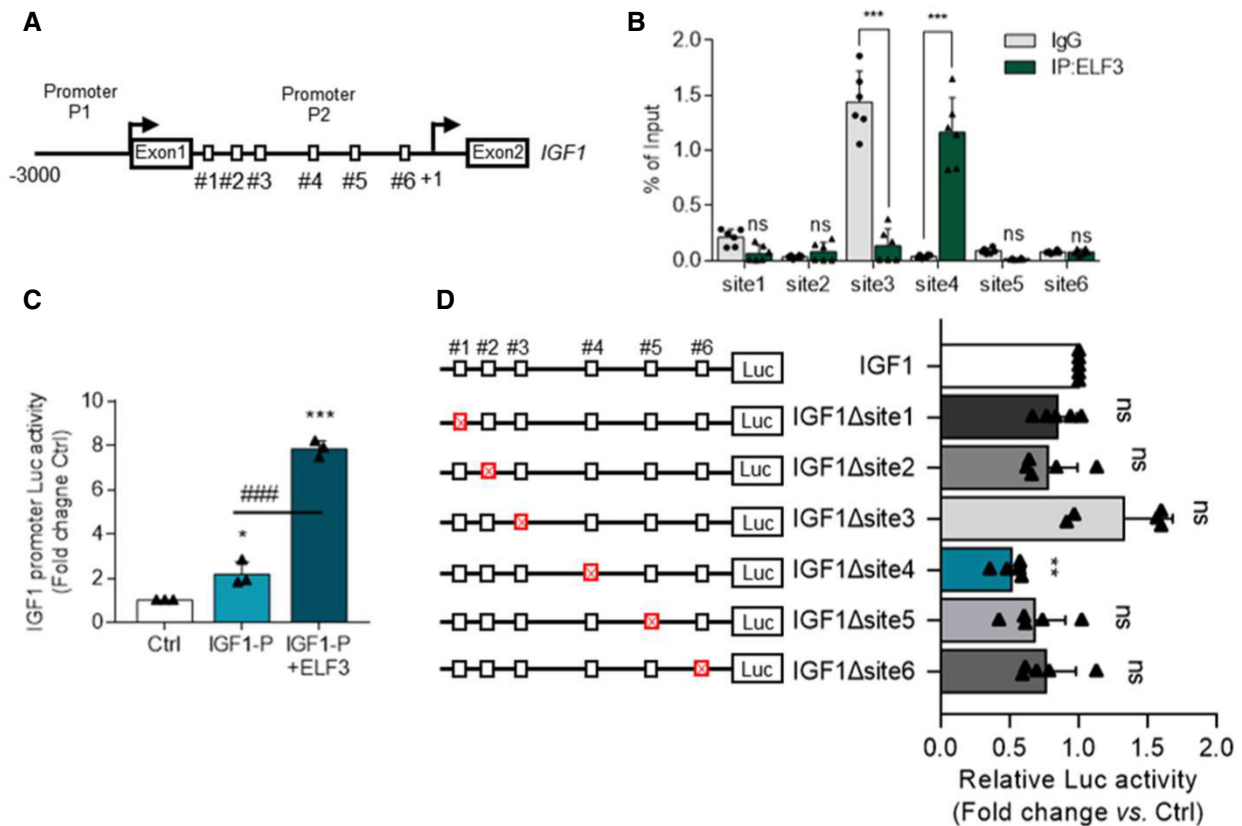


Figure 3. ELF3 transcriptionally regulated IGF1 expression.

- A** The schematic exhibits the six sites predicted as ELF3-responsive elements (EREs) in the IGF1 promoter.
- B** ChIP analysis was performed on the IGF1 promoter bound by ELF3 in SKOV3 cells. IgG was used as a negative control. Data were obtained from a qPCR evaluation ($n = 6$ independent repetitions).
- C, D** Luciferase reporter assay was performed in SKOV3 cells and normalized by Renilla. **(C)** SKOV3 cells were transfected with empty vector (Ctrl), IGF1 promoter (IGF1-P), or IGF1 promoter + ELF3 (IGF1-P + ELF3). **(D)** The left panel shows the various deleted IGF1 promoters used when co-transfecting SKOV3 cells with the ELF3 and the IGF1 promoters. The deleted IGF1 promoters lose each of the six predicted EREs. The right panel shows the degree of binding and transcriptional ability of ELF3 to the deleted IGF1 promoter through luciferase activity ($n = 5$ independent repetitions).

Data information: For all panels, data are expressed as mean \pm SD. **(B)** *** $P < 0.001$ vs. IgG; ns—not significant (two-way ANOVA, Sidak's). **(C)** * $P < 0.05$, *** $P < 0.001$ vs. Ctrl, ### $P < 0.001$ vs. IGF1-P (Kruskal–Wallis test, Dunn's). **(D)** ** $P < 0.01$ vs. IGF1-P (one-way ANOVA, Sidak's).

and microvascular sprouting (Chung *et al.*, 2010). We demonstrated that ELF3 transcriptionally regulated IGF1 expression (Fig 3) and that IGF1 indirectly regulated VEGF expression (Fig EV1). Therefore, to confirm the secretion of IGF1 and VEGF in accordance with the ELF3 expression in EOC cell lines, we performed dot blotting using conditioned media (CM). The secretion of IGF1 and VEGF increased in ELF3-overexpressed EOC cells and decreased in ELF3-silenced EOC cells (Figs 4A and EV2A). Next, transwell migration assay was used to evaluate the effect of the microenvironment changes of EOC cells in accordance with the ELF3 expression in ECs. The assay was performed as shown in scheme in Fig 4B. The proliferation of human umbilical vein endothelial cells (HUVECs) was significantly reduced when cultured in an environment with ELF3-silenced SKOV3 cells (Fig 4C). ELF3 overexpression in EOC cells significantly increased the migration of HUVECs, and ELF3 silencing remarkably reduced their migration (Figs 4D and EV2B). We then performed an *ex vivo* aortic ring assay to evaluate the effect of ELF3 expression on growing endothelial microvascular sprouts. Microvessel sprouting from the aortic ring incubated in the microenvironment of ELF3-overexpressed EOC cells was increased compared with the control (Figs 4E and EV2C). To understand how ECs were stimulated, we investigated the downstream signaling pathways of IGF1R and vascular endothelial growth factor receptor 2 (VEGFR2), which are known to be associated with EC proliferation and migration and vesicle permeability (Cross & Claesson-Welsh, 2001; Ding *et al.*, 2016; Teng *et al.*, 2016). Those signaling pathways were considerably activated in HUVECs incubated with the CM of ELF3-overexpressed EOC cells and remarkably attenuated in HUVECs cultured in the CM of ELF3-silenced EOC cells compared with the controls (Figs 4F and EV2D). The angiogenic effect was investigated to check whether HUVECs rescued paracrine effects when treated with CM of SKOV3-shCtrl or -shELF3 cells in the presence of recombinant VEGF. Upon treatment with recombinant VEGF, phosphorylation of VEGFR2 was increased compared with each control without recombinant VEGF, but phosphorylation of IGF1R was not changed. Phosphorylation of VEGFR2 was significantly attenuated in CM of SKOV3-shELF3 than in CM of SKOV3-shCtrl upon treatment with recombinant VEGF (Fig 4G). Thus, IGF1 induced by ELF3 promotes angiogenesis in two ways: via autocrine signaling in the EOCs and paracrine signaling in ECs.

Reducing ELF3 expression was highly effective at suppressing enhanced tumor angiogenesis under hypoxic conditions

Considering that the surrounding microenvironment becomes hypoxic as the tumor grows, we tried to investigate the ELF3-mediated changes in the angiogenesis markers of SKOV3 cultured under hypoxic conditions. Here, we confirmed that expression of both IGF1 and VEGF was increased accompanied by increased ELF3 expression under hypoxic conditions. However, where ELF3 was silenced despite exposure to a similar degree of hypoxia, expression and the secretion of IGF1 and VEGF did not show an upregulation pattern (Fig 5A). This result reflects that ELF3 is an important key regulator in EOC angiogenesis. By co-culturing SKOV3-shCtrl cells with HUVECs under hypoxic conditions, we also observed a remarkable increase in the migration and proliferation rate of HUVECs but found no significant changes when co-incubated with SKOV3-shELF3 cells (Fig 5B and C). Similarly, highly promoted microvascular sprouting from the aorta cultured in CM of SKOV3-shCtrl cells under hypoxic conditions was reduced in CM of SKOV3-shELF3 cells (Fig 5D). In the case of angiogenesis-related signaling pathways in HUVECs, IGF1R and VEGFR2 signaling pathways were significantly activated when incubated with CMs of SKOV3-shCtrl exposed to hypoxia but not when ELF3 was silenced in SKOV3. In particular, the phosphorylation of IGF1R showed a significant difference according to changes in ELF3-mediated IGF1 expression (Fig 5A and E). Moreover, an *ex vivo* Matrigel plug assay was used to evaluate the ELF3-dependent angiogenic capacity of EOC cells. We visually confirmed that the formation of new blood vessels derived from the existing ones was significantly lower in the SKOV3-shELF3-injected gel plug than in the SKOV3-shCtrl-injected gel plug (Fig 5F left). Hemoglobin content, a surrogate marker for functional blood flow, was also significantly lower in the SKOV3-shELF3-injected gel plug (Fig 5F right). Taken together, ELF3 in EOC plays a key role in regulating IGF1 expression and its secretion and in stimulating ECs to regulate angiogenic activities such as EC migration, proliferation, and microvascular sprouting.

ELF3 silencing attenuated angiogenesis and tumorigenesis in EOC-xenografted tumors

The effect of ELF3 expression on angiogenesis and tumor initiation ability was investigated by developing xenograft mouse models with

Figure 4. ELF3 was a key molecule inducing tumor angiogenesis by promoting IGF1 secretion in EOC cells.

- A The levels of secreted IGF1 and VEGF were analyzed using CMs from ELF3-overexpressed or ELF3-silenced EOC cells by dot blotting.
 B The schematic diagram of the method used to confirm the migration of HUVECs by the proteins secreted from EOC cells.
 C The proliferation of HUVECs under the same conditions as in (B) was measured using a WST-1 analysis ($n = 4$ independent repetitions).
 D Migration of HUVECs was observed using a transwell migration assay. Migrated HUVECs were stained with 2% crystal violet (scale bar, 500 μm). Images were quantified using ImageJ ($n = 3$ independent repetitions).
 E Microvascular sprouting ability was observed through an *ex vivo* aortic ring assay (scale bar, 100 μm). Aortic rings were co-stained with anti-CD31 (green) and anti- α SMA (red) antibodies. Arrowheads indicated sprouting vessels. The sprouting distances were quantified using ImageJ (Ctrl, $n = 3$; ELF3, $n = 4$ independent repetitions).
 F, G The changes in proteins of HUVECs were detected by western blotting. (F) HUVECs were cultured in CM of ELF3-overexpressed or -silenced SKOV3 cells. (G) HUVECs were cultured in CMs of SKOV3-sh Ctrl or -shELF3 cells treated or untreated with 10 ng/ml recombinant VEGF for 24 h. This blotting was performed and quantified in three independent experiments.

Data information: Data are expressed as the mean \pm SD. (C and D) $**P < 0.01$ vs. siCtrl (Student's *t*-test, two-tailed). (E) $***P < 0.001$ vs. Ctrl (Student's *t*-test, two-tailed). (F) $*P < 0.05$, $**P < 0.01$, $***P < 0.001$ vs. Ctrl or shCtrl (two-way ANOVA, Sidak's). (G) $*P < 0.05$, $***P < 0.001$ vs. shCtrl_non VEGF, $\#P < 0.05$, $###P < 0.001$ vs. shCtrl_VEGF (two-way ANOVA, Tukey's).

Source data are available online for this figure.

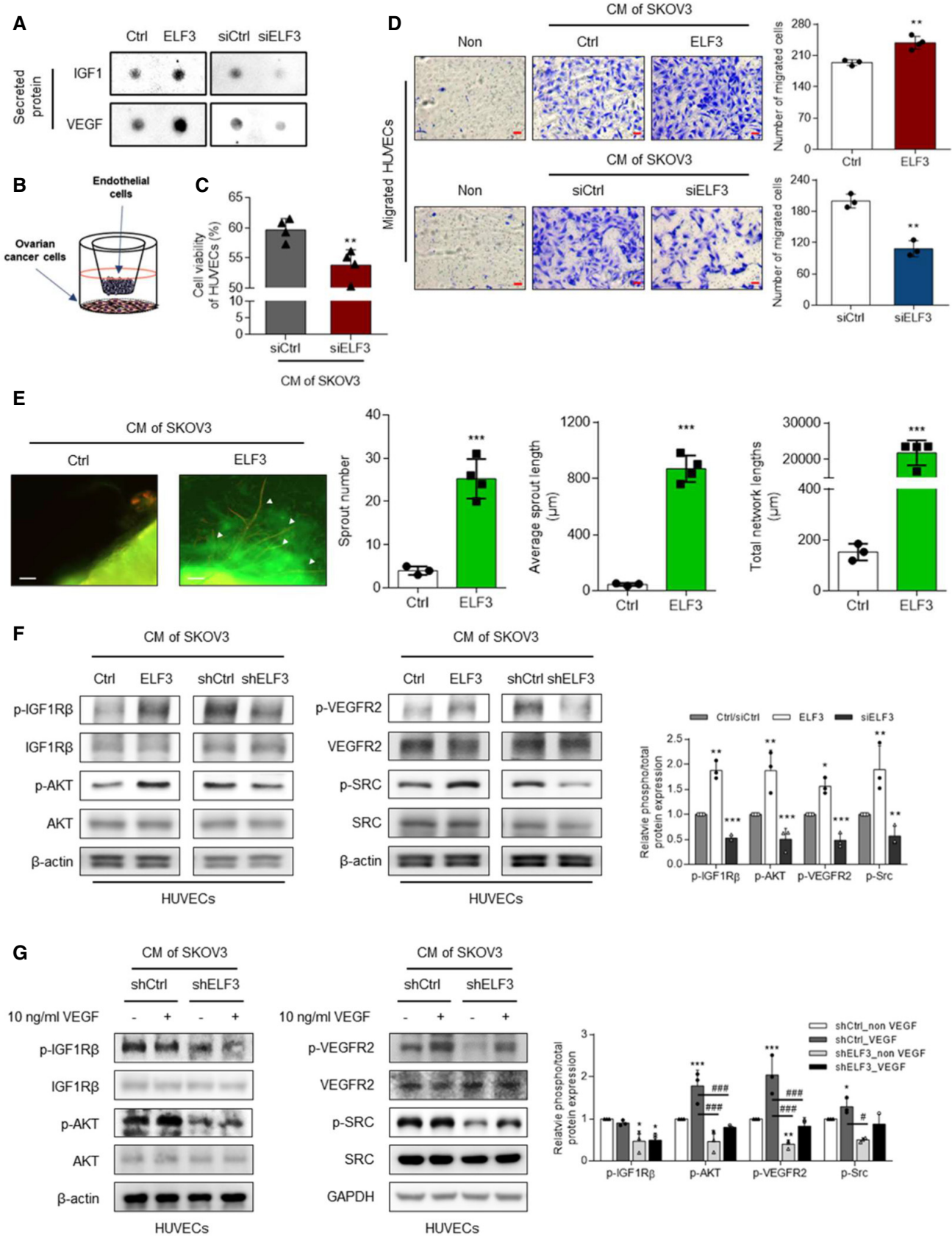


Figure 4.

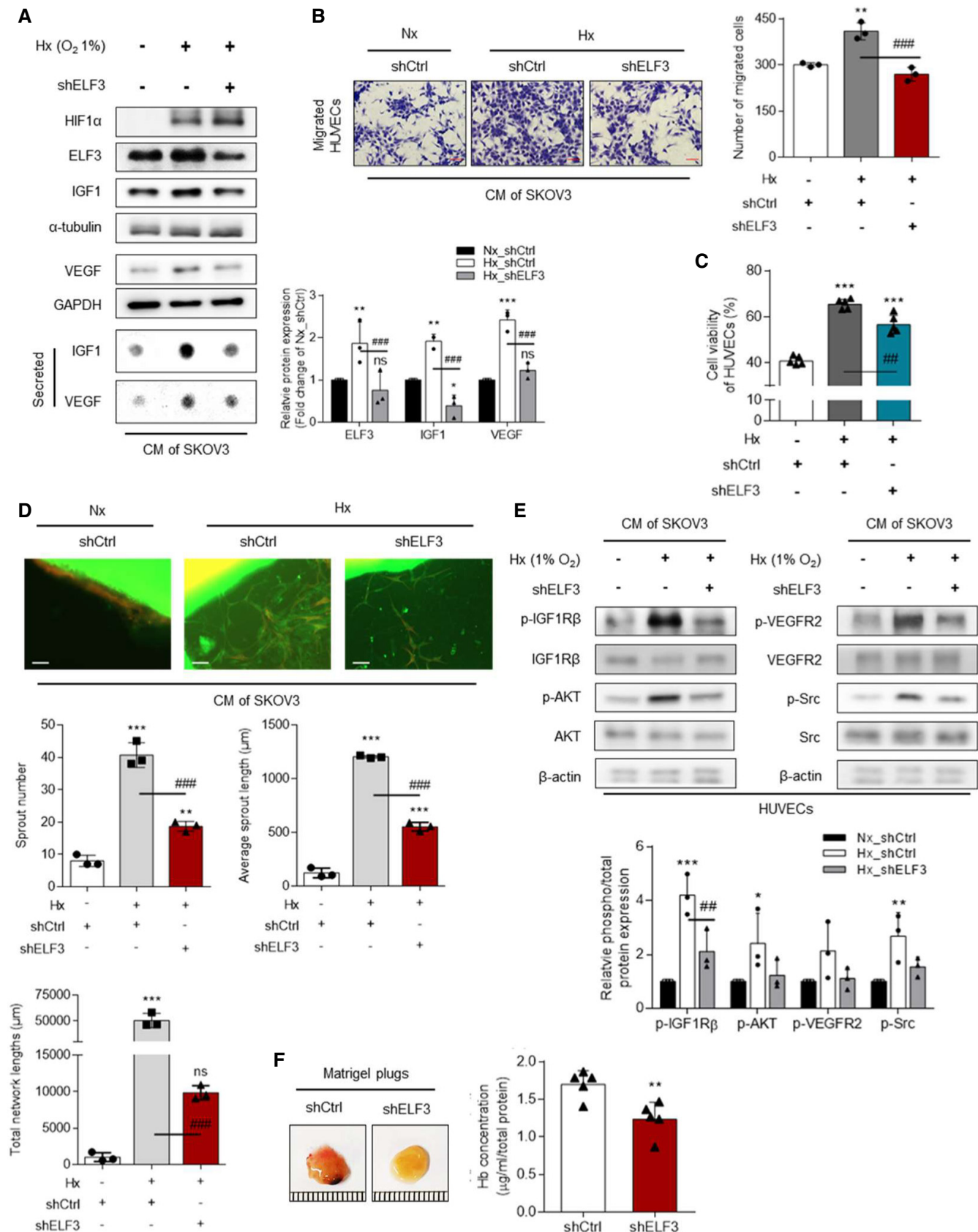


Figure 5.

Figure 5. Reducing ELF3 expression was highly effective at suppressing enhanced tumor angiogenesis under hypoxic conditions.

- A The changes in the expression and secretion of IGF1 and VEGF in SKOV3 when ELF3 was silenced under hypoxic conditions were compared through Western blotting and dot blotting, respectively. This blotting was performed and quantified in three independent experiments.
- B, C The migration and viability of HUVECs were measured after treatment with the CMs of SKOV3-shELF3 or SKOV3-shCtrl cells exposed to normoxic or hypoxic (1% O₂) conditions for 16 h. (B) Migrated cells were stained with 2% crystal violet. Images were quantified using ImageJ ($n = 3$ independent repetitions) (scale bar, 10 μ m). (C) Cell proliferation was measured using WST-1 assay.
- D Aortic rings were treated with CM of SKOV3-shCtrl or SKOV3-shELF3 cells exposed to normoxic or hypoxic conditions for 16 h (scale bar, 100 μ m). Aortic rings were co-stained with anti-CD31 (green) and anti- α SMA (red) antibodies. The sprouting distances were quantified using ImageJ ($n = 3$ independent experiment samples).
- E After treating HUVECs with CMs obtained from in (A), changes in protein levels in HUVEC were detected by Western blotting. This blotting was performed and quantified in three independent experiments.
- F *Ex vivo* vessel formation was assessed using Matrigel plug angiogenesis analysis. Matrigel plugs were excised when the mice were euthanized after 21 days (scale size, 1 mm). The hemoglobin (Hb) content was calculated by measuring absorbance at 540 nm. The Hb concentration is expressed by dividing by the total protein concentration of the Matrigel plug ($n = 5$ mice).

Data information: Data are expressed as mean \pm SD. (A–C) ** $P < 0.01$, *** $P < 0.001$ vs. shCtrl in Nx; ns—not significant; ## $P < 0.01$, ### $P < 0.001$ vs. shCtrl in Hx (A, two-way ANOVA, Tukey's; B, one-way ANOVA, Holm Sidak's; C, One-way ANOVA, Tukey's). (D) ** $P < 0.01$, *** $P < 0.001$ vs. shCtrl in Nx; ns—not significant; ### $P < 0.001$ vs. shCtrl in Hx (One-way ANOVA, Tukey's). (E) * $P < 0.05$, ** $P < 0.01$, *** $P < 0.001$ vs. shCtrl in Nx; ## $P < 0.01$ vs. shCtrl in Hx. (two-way ANOVA, Tukey's). (F) ** $P < 0.01$; vs. siCtrl (Student's *t*-test, two-tailed).

Source data are available online for this figure.

SKOV3-shELF3 or SKOV3-shCtrl cells in immunodeficient nude mice. As a result, SKOV3-shCtrl cells formed tumors in seven, six, and none out of seven mice when injected with 5×10^6 cells, 5×10^5 cells, and 5×10^4 cells, respectively. However, SKOV3-shELF3 cells formed tumors in three, two, and none out of seven mice when injected with 5×10^6 cells, 5×10^5 cells, and 5×10^4 cells, respectively (Fig 6A). In Fig 6B and C, tumors started to grow on day 17 after transplantation of 5×10^6 SKOV3-shCtrl cells and on day 34 after transplantation of 5×10^6 SKOV3-shELF3 cells. SKOV3-shELF3 cell-xenografted tumors showed a slower growth rate than that of SKOV3-shCtrl cells. Tumors transplanted with 5×10^5 SKOV3-shCtrl cells started to grow on day 20, whereas tumors transplanted with 5×10^5 SKOV3-shELF3 cells started to grow on day 45. 5×10^5 SKOV3-shCtrl tumors showed rapid growth after 38 days, and 5×10^5 SKOV3-shELF3 tumors showed much slower growth rates. The weight of SKOV3-shELF3 tumors slightly decreased compared with SKOV3-shCtrl tumors, although there was no significant difference in tumor weights between the two groups (Fig 6D). Through IHC staining, we confirmed that IGF1 expression in SKOV3-shELF3 tumors was quite low compared with SKOV3-shCtrl tumors (Fig 6E and F). The expression of Ki-67, a proliferation marker, was also significantly reduced in SKOV3-shELF3 tumors (Fig 6E and G). Furthermore, the microvessel density was significantly lower in the SKOV3-shELF3 tumors than in the SKOV3-shCtrl tumors (Fig 6H and I). These results demonstrate that ELF3 plays an essential role in regulating angiogenesis and tumorigenesis in EOC.

Discussion

The ETS family, including Ets1, Ets2, and ELK3, has been studied for its association with angiogenesis through the regulation of gene expression in ECs (Meadows *et al*, 2011; Heo & Cho, 2014; Chen *et al*, 2017; Hofmann & Heineke, 2019). Considering that angiogenesis is activated by a hypoxic microenvironment that occurs when EOC tumors grow excessively (Bergers & Benjamin, 2003), we sought to find a transcription factor overexpressed in EOC under hypoxic conditions and regulate its expression within EOC to obtain antiangiogenic and anticancer effects. Among the 51 TFs overexpressed by hypoxia, ELF3 was the most highly expressed gene in OCs. Similar patterns were also observed in carcinomas such as breast, lung, and prostate cancers, in which ELF3 is known to act as an oncogene (Eckel *et al*, 2003; Longoni *et al*, 2013; Kar *et al*, 2017; Zhang *et al*, 2021; Fig EV3). Thus, we expect that the significance of ELF3 as an oncogene to induce angiogenesis may not be restricted to EOC only, and may be noticeable in some other cancer subtypes. A recent multiomics analysis revealed that ELF3 is a target gene for HIF-1 α (Andrysik *et al*, 2021). As HIF-1 α expression is naturally increased under hypoxic condition, accompanied overexpression of ELF3 can be interpreted as an outcome of enhanced transcriptional activity of HIF-1 α . To experimentally confirm the results of this study, we predicted the hypoxic response element (HRE) region of the ELF3 promoter to refer EPD analysis ($P < 0.0001$), and confirmed that HIF-1 α directly regulated the

Figure 6. ELF3 silencing attenuated angiogenesis and tumorigenesis in EOC-xenografted tumors.

- A For *in vivo* tumorigenicity assays, mice were injected subcutaneously with 5×10^6 , 5×10^5 , and 5×10^4 SKOV3-shCtrl or SKOV3-shELF3 cells, respectively. Mice were euthanized on day 52 after transplantation ($n = 7$ mice per group).
- B After implantation into mice with subcutaneous injection of SKOV3-shCtrl cells or SKOV3-shELF3 cells, tumor volumes were measured every 3–4 days from the time of tumor growth. As provided in (A), the tumor growth curve was analyzed statistically by measuring only the grown tumor.
- C Images of the generated tumors excised from mice euthanized on day 52 are shown.
- D As in (A) and (C), only the grown tumors were weighed and analyzed statistically.
- E–I IHC analysis of SKOV3-shCtrl or -shELF3 tumor sections was performed with tumors pooled from both 5×10^6 and 5×10^5 groups, and IHC results were statistically analyzed. (E and H) In ELF3, IGF1, ki67, CD31 staining, nuclei are stained with hematoxylin, and each protein is stained with DAB. (F) ELF3 and IGF1 were quantified with the IHC profiler in ImageJ. (G) Ki-67 positive cells were normalized to the hematoxylin-stained area and expressed as percentages. (I) Microvessel density was quantified with the IHC profiler in ImageJ.

Data information: For all panels, data are presented as mean \pm SD. (B and D) * $P < 0.05$; ** $P < 0.01$; *** $P < 0.001$ (two-way ANOVA, Sidak's). (G and I) * $P < 0.05$; *** $P < 0.001$ (Student's *t*-test, two-tailed).

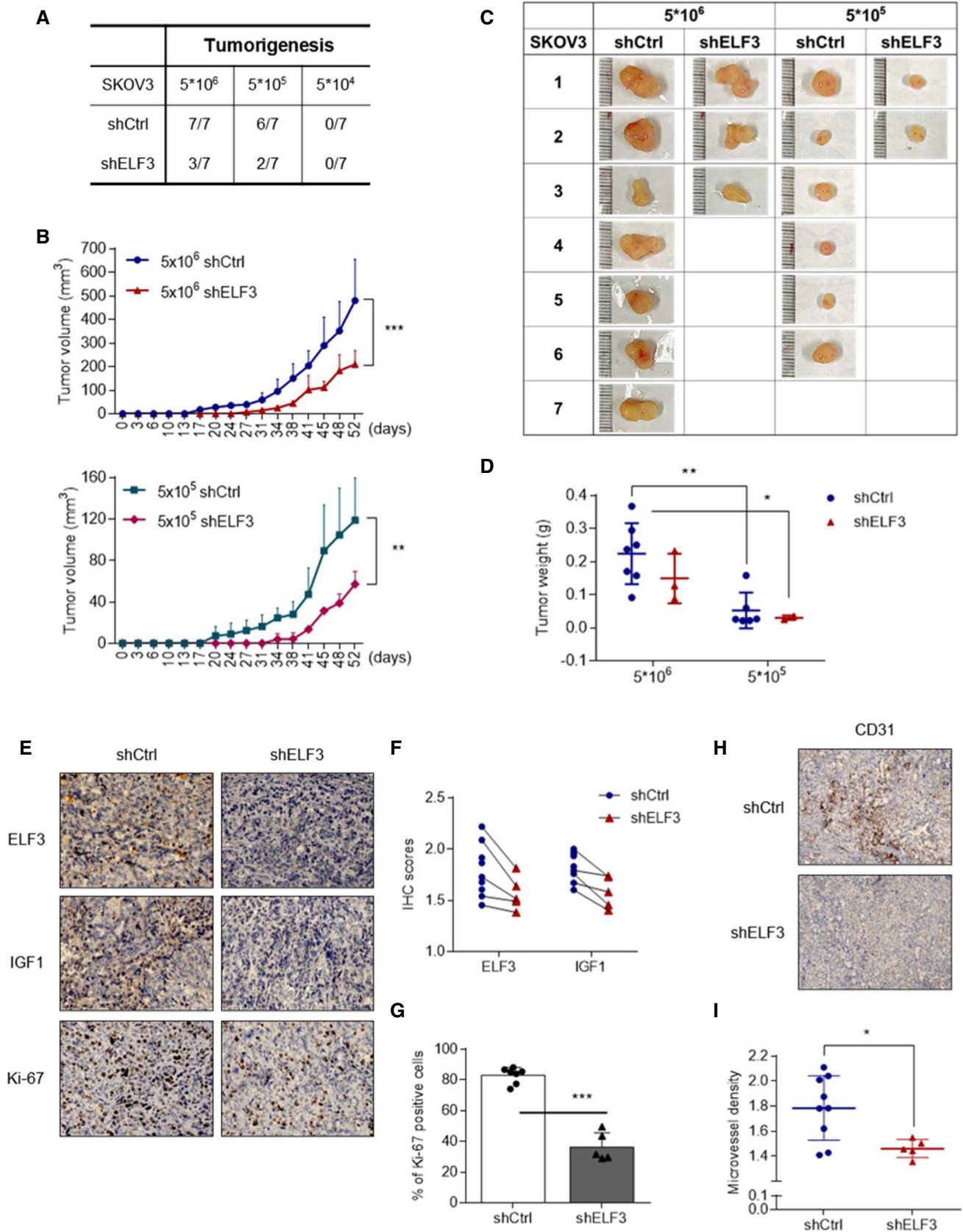


Figure 6.

expression of ELF3 through ChIP, luciferase reporter gene analysis, and western blotting (Fig EV4).

We used an angiogenic antibody array analysis to identify angiogenic factors that show a positive correlation with ELF3 and finally found that ELF3 transcriptionally regulates IGF1. The *IGF1* promoter consists of two classes: class I contains exon 1 upstream of the TSS, and it is driven by the P1 promoter, whereas class II starts transcription from exon 2 and is driven by the P2 promoter (Ouni et al, 2016). When analyzing IGF1 promoter through EPD, we found that six predicted EREs in the P2 promoter but no EREs in the P1 promoter (reference; NG_011713). We verified that IGF1 mRNA levels are indeed regulated by ELF3 using primers targeting exon1 and exon2 of IGF1, respectively. Along with the ELF3 overexpression, only the mRNA level of IGF1 exon 2 increased. No changes were observed in exon1 (Fig EV5). In this study, we newly elucidated that ELF3 increases the expression and secretion of proangiogenic factors, such as IGF1 and VEGF in EOC cells. They subsequently activate ECs through receptor tyrosine kinase pathways to promote angiogenic effects such as migration, proliferation, sprouting, and permeability. Typically, IGF1 induces the development and progression of various tumors through paracrine/autocrine signaling (Ding et al, 2016; Teng et al, 2016) and promotes the proliferation and survival of ECs (Bach, 2015; Lin et al, 2017). Moreover, IGF1 has been reported to play a critical role in activating the PI3K/AKT signaling pathway, leading to migration, tube formation, and the production of the vasodilator NO in ECs (Bach, 2015; Lin et al, 2017).

Tumor angiogenesis is induced by downstream signaling such as PI3k/Akt and Src when tyrosine kinase receptors, such as IGF1R and VEGFR2, are activated by angiogenic factors in ECs (Gerber et al, 1998; Eliceiri et al, 1999; Takahashi et al, 1999; Chen & Han, 2008). Each signaling pathway is involved in an extensive biological process in ECs. The Src pathway is involved in vascular permeability regulation and cytoskeletal rearrangement. The PI3k/AKT pathway regulates cell survival and proliferation. Moreover, we also evaluated the downstream signaling of IGF1R and VEGFR2 in HUVECs cultured in CM of SKOV3-shCtrl or -shELF3 cells exposed to hypoxia or normoxia, and we did not observe increased expression and secretion of IGF1 under hypoxia, where ELF3 was silenced (Fig 5A). Along with changes in ELF3 expression levels, angiogenic activities and signaling, particularly IGF1R signaling, were significantly affected (Fig 5B–F). That is additional evidence indicating that ELF3 directly regulates IGF1. Considering that IGF1 indirectly regulates VEGF expression (Fig EV1A–C), the reduced VEGF is considered to be an effect following IGF1 reduction. This phenomenon may explain the decreased VEGFR2 downstream signaling in the CM of SKOV3-shELF3 compared with the control despite the artificial addition of VEGF (Fig 4G). These results confirmed that tumor angiogenesis was greatly affected by the expression level of ELF3, which activates IGF1.

In summary, we used a variety of experimental techniques to discover and confirm that ELF3 has an important function in regulating tumor angiogenesis. ELF3 is overexpressed under hypoxia. ELF3 acts as a direct TF of IGF1 and induces angiogenesis by promoting EC proliferation and migration. Our results highlight that ELF3 plays an essential role in promoting tumor angiogenesis by inducing synergistic expression of IGF1 under hypoxic conditions. ELF3 has the potential to be an innovative therapeutic target to inhibit progressive EOC-induced tumor angiogenesis.

Materials and Methods

Cell culture, hypoxic incubation, and transfection

The human EOC cell lines; SKOV3, OVCAR3, and Caov3 were cultured in McCoy's 5A Medium, Modified (McCoy's 5A; LM 005-01, Welgene Inc.), Roswell Park Memorial Institute 1640 medium (RPMI 1640; LM 001-01, Welgene Inc.), and Dulbecco's Modified Eagle Medium (DMEM; LM 001-05, Welgene Inc.), respectively. Each medium was supplemented with 10% FBS (35-015-CV, Corning Inc.) and 1% penicillin-streptomycin (sv30010, HyClone). Human umbilical vein endothelial cells (HUVECs) (PCS-100-010, ATCC) were cultured in an M199 medium containing 20% FBS and 1% penicillin-streptomycin, and 3 ng/ml bFGF (#13256029, Thermo Fisher Scientific). OVCAR3 and HUVECs were obtained from Dr. Seung Bae Rho at the National cancer center (NCC, Korea). SKOV3 and Caov3 were purchased from the Korean Cell Line Bank (KCLB, Korea). HUVECs were cultured on a 100-mm culture dish (#20100, SPL) coated with 0.1% gelatin (G1890, Sigma-Aldrich). All cells were grown in a humidified atmosphere at 37°C at gas compositions of 20% O₂/5% CO₂ for normoxic conditions and 1% O₂/5% CO₂/94% N₂ for hypoxic conditions for 16 h in a hypoxic chamber (Don Whitley Scientific, UK). Chemically hypoxic conditions were incubated in a medium treated with 100 μM CoCl₂ for 6 h in a humidified atmosphere at 37°C.

All cells were transfected with 0.5–1.0 μg plasmid DNA using jetPrime® (#101000046, Polyplus) according to the manufacturer's protocol for transient overexpression of the protein. For transient knockdown of the protein, 100 nM siRNA of ELF3 (siELF3) (BIONEER, Korea) or 300 nM siRNA of IGF1 (siIGF1) (BIONICS, Korea) were transfected with Lipofectamine 2000 (#11668019, Invitrogen) according to the manufacturer's instructions. To stably knockdown ELF3 using jetPrime®, a lentivirus particle was generated in HEK293T that was transfected with pRSV-Rev, pMDLg/pRRE (packaging vector), pCMV-VSVG (envelope vector), and pLKO.1 vector inserted with the sequence of shCtrl or shELF3 (TRCN0000013865, Merck). A medium containing a lentivirus particle was harvested after three days of incubation and was centrifuged at 2,000 rpm for 5 min. The supernatants were filtered with a 0.45-μm mixed cellulose ester syringe filter (25AS045AS, ADVANTEC). 1.5 × 10⁵ SKOV3 cells per well were seeded in 6-well plates to reach about 50% confluence by incubation for 24 h. It was then treated with 1 ml of filtrated medium and polybrene was added to a final concentration of 8 μg/ml. After three days, the infected cells were transferred to a 100-mm culture dish and were selected for two weeks in a medium containing 3 μg/ml puromycin. The selected cell was named SKOV3-shCtrl or SKOV3-shELF3.

Plasmid DNA and reagent

Plasmid DNA constructs were generated for different types of experiments, including alteration of the level of target proteins and luciferase reporter gene assay. ELF3 (NM_001114309.1) was inserted into the EcoRI/KpnI site of p3Xflag-Myc-CMV26 and was used to enhance the ELF3 level. siELF3 or shELF3 were purchased for Bioneer or Sigma, respectively, to silence the ELF3 level. In luciferase reporter gene assay, six repeats of the predicted ELF3 binding site (EBS) were cloned into a pGL3-basic [Rluc-TK] vector using a

KOD-plus-mutagenesis kit (SMK-101, Toyobo). The pGL3-basic [Rluc-TK] vector was created by inserting the renilla-expressing portion of the Rluc-TK vector into the pGL3-basic vector to normalize the transfection efficiency. The pGL3-basic vector was obtained from Prof. Eun Sook Hwang at Ewha Womans University (Korea). The hypoxia-responsive element (HRE) of the *ELF3* promoter and EBS of the *IGF1* promoter were provided by customer service of Cosmogenetech Co. Ltd (Korea). The binding sites for each promoter were predicted at a cutoff < 0.001 using EPD (Eukaryotic Promoter Database). As the HRE sites of the *ELF3* promoter are located at -2,327 and -2,324 ($P = 0.001$), the *ELF3* promoter was constructed from -3,000 to -2,000 bp based on TSS. The ERE site of the *IGF1* promoter was constructed from -3,000 to 0 bp based on TSS, because it was predicted at -1865 (site 1, #1), -1697 (site 2, #2), and -1506 (site 3, #3), -1065 (site 4, #4), -703 (site 5, #5), and -393 (site 6, #6). To precisely determine which site of the *IGF1* promoter is responsible for *ELF3* binding, each binding site was deleted from the *IGF1* promoter to verify the site where *ELF3* acts as a TF. The primers used for cloning are shown in Table EV2.

Chromatin immunoprecipitation (ChIP) assay

SKOV3 cells were seeded in a 150-mm culture plate (#11150, SPL) and cultured overnight to reach 80% confluence. SKOV3 cells were then prepared according to the experimental conditions. 1% formaldehyde was added to the medium of each plate followed by shaking at room temperature (RT) for 10 min. Glycine was added to each plate to a final concentration of 125 mM, and the plate was shaken at RT for 10 min to deactivate excess formaldehyde. After removing the medium, the cells were washed twice with ice-cold phosphate-buffered saline (PBS) and harvested with 1 ml ice-cold PBS containing a 1× protease inhibitor cocktail (P3100-005, Gendepot) followed by centrifugation at $3,000 \times g$ at 4°C for 5 min. Then, the cell pellet was resuspended with 300 µl of lysis buffer (5 mM Tris-pH 8.0, 85 mM KCl, 0.5% NP-40) containing 1× protease inhibitors and vortexed for 15 s and incubated for 10 min on ice. The cell lysate was centrifuged at $9,000 \times g$ for 5 min at 4°C to obtain a nuclear pellet. The pellets were resuspended with 300 µl MNase digestion buffer working solution (50 mM Tris-pH 7.6, 1 mM CaCl₂, 0.2% Triton X-100) containing 1 mM DTT, and 0.75 µl micrococcal nuclease (10 U/µl) (#1862753, Thermo Fisher Scientific) was added and held in a 37°C water bath for 15 min with vortexing every 5 min. The samples were centrifuged at $9,000 \times g$ for 5 min at 4°C. The remnant pellet was suspended with nuclear lysis buffer (5 mM Tris-pH 8.0, 85 mM KCl, 0.5% NP-40) containing 1× protease inhibitors and was incubated on ice for 15 min. The suspended lysate was centrifuged at $9,000 \times g$ for 5 min at 4°C. The supernatant was transferred to a new centrifuge tube. The collected lysate was diluted to 1:5 ratio with ChIP dilution buffer (0.01% SDS, 1.1% Triton X-100, 1.2 mM EDTA, 16.7 mM Tris-HCl pH 8.1, and 167 mM NaCl). Immunoprecipitation (IP) was performed by incubating 5 µg of each primary antibody (HIF-1α antibody or *ELF3* antibody) or IgG antibody (#1862244, Thermo Fisher Scientific) with the diluted lysate at 4°C overnight with constant rotation. The IgG antibody was used as a negative control protein. Then, 20 µl of ChIP-beads (#26159, Thermo Fisher Scientific) were added to each sample and incubated for 3 h at 4°C with constant

rotation. The immunoprecipitates were washed sequentially with low salt wash buffer (0.1% SDS, 1% Triton X-100, 2 mM EDTA, 20 mM Tris-HCl pH 8, 150 mM NaCl), high salt wash buffer (0.1% SDS, 1% Triton X-100, 2 mM EDTA, 20 mM Tris-HCl pH 8, 500 mM NaCl), and TE buffer (10 mM Tris-HCl, 1 mM EDTA pH 8). The protein-DNA complex was eluted in ChIP elution buffer (1% SDS, 0.1 M NaHCO₃) containing 300 mM NaCl and 1 µl RNase. The eluate was incubated overnight at 65°C to generate reverse cross-linking. ChIP DNA was incubated for 90 min at 60°C after treating the proteinase K solution, (#1862780, Thermo Fisher Scientific). ChIP DNA was precipitated using a gel extraction kit (CMG0112, Lobopass™) according to the manufacturer's protocol. The purified ChIP DNA was dissolved in ultrapure water, and RT-qPCR was conducted. The primers used for RT-qPCR are shown in Table EV3.

Real-time qPCR (RT-qPCR)

According to each manufacturer's protocol, total RNA was isolated from cells using Tri-RNA reagent (FATRR001, FAVORGEN Biotech Crop.), and complementary DNA (cDNA) was synthesized with a PrimeScript™ RT reagent kit (RR037A, Takara Bio Inc.). RNA to be identified was quantified using the SensiFAST™ SYBR No-ROX kit (BIO92020, Bioline). The results were measured using the CFX96 Real-Time PCR detection system (Bio-Rad, Korea). The primers used for RT-qPCR are shown in Table EV3.

Luciferase reporter gene assay

The luciferase reporter gene assay used two types of vectors. One is a pGL3-basic vector, and the other is a pGL3-basic [Rluc-TK] vector. A β-galactosidase-CMV vector was used to normalize the transfection efficiency of the pGL3-base vector. The *ELF3* promoter containing HRE (indicated as *ELF3-P*) was cloned into the pGL3-basic vector. The *IGF1* promoter containing EBS (*IGF1-P*) or predicted EBS repeat sequence were cloned into the pGL3-basic [Rluc-TK] vector. SKOV3 cells were seeded in a 60-mm culture dish and transfected with 1 µg of each plasmid for 24 h. According to each manufacturer's protocol, *ELF3-P/pGL3-basic* and β-galactosidase-CMV vectors were used for the luciferase assay system (E1500, Promega) and the Galacto-Light Plus™ System (T1007, Thermo Fisher Scientific). *IGF1-P/pGL3-basic [Rluc-TK]* and *EBS/pGL3-basic [Rluc-TK]* were used to measure luciferase activity using the Dual-Glo® Luciferase assay system (E2940, Promega). Each luciferase activity was measured using a Tecan Infinite® 200 PRO microplate reader (Tecan, Tecan Group Ltd, Switzerland) equipped at Ewha Drug Development Research Core Center.

Western blot analysis

Whole-cell lysates were washed twice with PBS and suspended in RIPA buffer (#9806, Cell Signaling Tech) containing 1 mM PMSF and 1× protease inhibitor with incubation for 30 min on ice and vortexing for 15 s every 10 min. The amount of protein in lysates was estimated using a Pierce™ BCA Protein Assay Kit (#23225, Thermo Fisher Scientific). Levels of angiogenic factors secreted into conditioned media (CM) were checked using dot blots. Dot blot analysis was performed by spotting the same volume CM on the

nitrocellulose (NC) membrane (DG-NC3000, DoGenBio) several times. Then, 30–40 μg of proteins were resolved using Tris–Glycine SDS–PAGE, transferred to a 0.2- μm PVDF membrane (#1212639, Pall Life Science), and immunoblotted with specific antibodies. After washing with TBS-T, membranes were incubated with the horseradish peroxidase-conjugated secondary antibodies (GTX213110 or GTX213111, GeneTex) for 1 h at RT. The images were detected using an LAS-3000 equipped at Ewha Drug Development Research Core Center and were analyzed using Multi-Gauge Software (Fuji Photo Film Co. Ltd., Japan). The primary antibodies used in this study are shown in Table EV4.

Animal studies

BALB/c nude mice (CanN. Cg-Foxn1 nu, 4 weeks old) and in C57BL/6N (8 weeks old) were purchased from ORIENT BIO (Korea). The animal studies were approved by the Institutional Animal Care and Use Committee (IACUC) of Ewha Womans University [IACUC20-031]. The conditions of the mouse housing are constant temperature (20–22°C) and humidity (50–60%) under a light-dark cycle (12/12 h) and free access to food and water. Before the experiment, animals were randomly divided into groups according to the experimental design.

Aortic ring assay and immunofluorescence staining

Angiogenic sprouting was assessed using the aortic ring assay, which quantified the angiogenic blood vessels growing in a portion of the aorta (Baker *et al*, 2011; Kapoor *et al*, 2020). The thoracic aorta was dissected in C57BL/6N mice. The isolated aorta was washed on ice with DMEM/F12 medium (LM002-101, Welgene) containing 1% penicillin/streptomycin and was cut into 1-mm ring fragments. Sectioned aortic rings were starved overnight at 37°C and 5% CO₂ in DMEM/F12 medium containing 1% penicillin/streptomycin and then embedded in a growth factor-reduced Phenol-Red Free Matrigel[®] Matrix (#356231, Corning) mixed in a 1:1 ratio in each CM in 96-well plates. Embedded rings were incubated for 7 days at 37°C with 5% CO₂ in each CM.

For immunofluorescence staining of the aortic rings (Baker *et al*, 2011), the culture medium was aspirated, and each well of the plate was washed with PBS. The aortic ring was incubated in 100 μl of 4% formaldehyde for 30 min at RT to fixate the aortic ring. After removing the fixative and washing three times with PBS, the aortic rings were permeabilized using permeation buffer (0.25% (vol/vol) Triton X-100 in PBS) for 15 min at RT. The primary antibodies of anti-CD31 for labeling ECs and anti- α -SMA for labeling support cells were prepared with PBEC buffer (0.1 mM MnCl₂, 1% (vol/vol) Tween-20 in PBS). The aortic rings were incubated overnight at 4°C in 50 μl of primary antibody solution per well, then washed three times for 15 min with PBS containing 0.1% (vol/vol) Triton X-100. Next, the secondary antibody was prepared in PBEC buffer by selecting a host suitable for the primary antibody, and the aortic rings were incubated at RT for 2 h in the secondary antibody solution. Then, the antibody solution was removed and washed three times with PBS containing 0.1% (vol/vol) Triton X-100. After washing once with distilled water, images were taken using a microscope Observer7 (Apotome) (Carl Zeiss, Germany). ImageJ was used to quantify microvessel sprouting.

Matrigel plug assay and hemoglobin measurement

The angiogenesis *ex vivo* analysis was assessed using a Matrigel plug assay (Lung & Lung, 2012). Each of 5×10^6 SKOV3-shCtrl cells or SKOV3-shELF3 cells was mixed with 450 μl of Matrigel and injected subcutaneously into the flanks of 5-week-old BALB/c nude mice. Five mice were used for each experimental condition. On day 21, mice were euthanized and Matrigel plugs containing SKOV3-shCtrl or shELF3 cells were collected. All Matrigel plugs were detached from the mice and digitally photographed. After freezing all Matrigel plugs, 20 mg of the fresh plugs were resuspended in 300 μl of lysis buffer (20 mM HEPES, 1% Triton-X100, 0.15 M NaCl 1 mM EDTA 10% glycerol, 1 mM EGTA, 5 mM NaF, inhibitor cocktail, 0.5% NP-40, 1% PMSF, 1 mM Na₃VO₄) on ice using a homogenizer (Cole-Parmer, USA). The homogenate was centrifuged for 10 min at 6,000 rpm at 4°C. The supernatant was collected, and the protein concentration was determined using BCA protein assay. Drabkin's reagent/Brij 35 solution was prepared by adding a vial of Drabkin's reagent (D5941-6VL, Sigma-Aldrich) into 1 l of water containing 0.5 ml of 30% Brij 35 solution (B4184-10ML, Sigma-Aldrich). In parallel, a stock solution of hemoglobin at a concentration of 10 mg/ml was resuspended in the lysis buffer, and an eight-point standard curve was made using 2-fold serial dilutions of hemoglobin. To 10 μl of each sample or standard in each well, 100 μl of Drabkin's reagent/Brij 35 solution was added in triplicate experiments followed by incubation for 15 min at RT. The absorbance intensity of each well was detected at 540 nm by Tecan. The hemoglobin concentration of the sample was normalized by the protein concentration as determined by a BCA protein assay kit.

Subcutaneous tumorigenesis assay

SKOV3-shCtrl or -shELF3 cells were resuspended in a mixture of PBS at 5×10^6 , 5×10^5 , or 5×10^4 cells/100 μl . SKOV3-shCtrl (left) or -shELF3 (right) cells were then injected subcutaneously into respective flanks of mice. Seven mice per group were used for this experiment. Tumor volumes were measured every 3–4 days. After euthanizing the mouse, the tumor was surgically separated, weighed, photographed, fixed in 4% paraformaldehyde solution, and sent to K.C.F.C Chemical (Korea) to make a section with paraffin-embedded tissue.

Immunohistochemistry (IHC) staining

Formalin-fixed paraffin-embedded tissues were sectioned into 5- μm segments. After warming the section to dissolve paraffin, it was washed 3 times for 5 min with xylene to remove paraffin. Sections were rehydrated in the following ethanol grade steps (2 \times 10 min in 100% ethanol, 5 min in 95% ethanol, 3 min in 70% ethanol, 3 min in 50% ethanol). Slides were subjected to antigen retrieval by boiling the slides intermittently for 20 min using a microwave in 1 \times Antigen Retrieval Buffer (ab93678, Abcam). The slides were left at RT for about 30 min to cool, and washed by immersion in distilled water for 5 min. To block endogenous peroxidase activity, sections were incubated in REAL peroxidase blocking solution (s2023, Agilent Technologies) for 15 min. Sections were subjected to nonspecific binding blocking and antibody staining using the VECTASTAIN[®] Elite ABC-HRP Kit (PK-6101 (Rabbit) or PK-6102

(Mouse), VECTOR Laboratories) according to the manufacturer's instructions. Sections were incubated with normal blocking serum buffer for 30 min and were then incubated with primary antibody overnight at 4°C in a humid chamber. The primary antibodies used in this study are presented in Table EV4. After washing 3 times in PBS for 3 min each, the tissue sections were incubated with biotinylated secondary antibodies for 1 h at RT. While waiting for the previous step, an ABC reagent solution was prepared by mixing 100 µl reagent A and 100 µl reagent B in 5 ml of normal blocking serum solution followed by activating at 37°C for 30 min. After washing 3 times with PBS for 3 min each, the sections were incubated with ABC reagent solution for 30 min. Sections were incubated in DAB working solution (150 µl KPL Tris buffer, 100 µl KPL DAB solution, and 100 µl KPL peroxide solution in 5 ml of distilled water) according to the manufacturer's instructions (#5510-0031, SeraCare Life Sciences, Inc.). DAB reaction times were determined appropriately for each antibody. After washing 3 times with distilled water for 3 min each, the tissue sections were stained with Mayer's hematoxylin (HMM999, ScyTek Laboratories) for 1 min and washed with running water for 10 min. Finally, the sections were dehydrated in the following steps (3 min in 70% ethanol, 3 min in 95% ethanol, 3 min in 100% ethanol, and 3 min in xylene) and mounted with mounting solution (SP15-100, Fisher Chemical). The staining intensity of the protein was quantified using Fiji software.

Conditioned medium (CM)

Each EOC cell line (SKOV3, OVCAR3, and Caov3) was seeded in a 60-mm culture dish (#20060, SPL) to 80% confluence, and it was incubated for 24 h. Each cell line was transfected with ELF3 or siELF3 for 5 h using the transfection reagent. After washing with PBS, it was replaced with a serum-free medium. After 20 h of incubation, a conditioned medium (CM) was collected and centrifuged at 2,000 rpm for 2 min at 4°C to remove cell debris. SKOV3-shCtrl or SKOV3-shELF3 cells were seeded in a 60-mm culture dish and incubated for 24 h. After washing with PBS and replacing it with serum-free media, SKOV3-shELF3 cells were incubated in hypoxic conditions (1% O₂) for 16 h, and SKOV3-shCtrl cells were incubated under normoxic or hypoxic conditions. Each CM was used to measure secreted angiogenic factors and to investigate tumor angiogenesis *in vitro* or *ex vivo*.

Transwell migration assay

Cell migration assays were conducted using a Transwell® (#3422, Corning Inc.). All cells were seeded in 24-well plates (#30024, SPL) and were incubated for 24 h. After each cell was transfected with overexpressed or silenced ELF3 for 5 h, it was replaced with serum-free media. HUVECs were then seeded in a transwell chamber in serum-free media and incubated together with transfected cells for 24 h (Fig 4B). After washing twice with PBS, migrating cells were fixed with 4% formaldehyde in PBS for 10 min. After washing twice with PBS, cells were treated with 100% methanol for 20 min and were stained with 1% crystal violet solution for 30 min. After the stained cells were sufficiently washed with PBS, the unmigrated cells remaining on the upper surface of the plate were thoroughly removed using a cotton swab and were then air-dried. The images

of stained cells were taken using an AXIOSCOPE (Carl Zeiss, Germany) microscope.

Cell viability assay

Human umbilical vein endothelial cells were seeded in 96-well plates and cultured for 24 h. Following washing with PBS, the cells were replaced with CM and incubated for 24 h. Then, 5 µl of Quanti-Max™ (QM10000, BIOMAX) was added to each well, and the cells were incubated for about 3 h at 37°C. The absorbance was measured at 450 nm using Tecan. Absorbance values are expressed relative to DMSO-treated controls and are shown as percentages.

Angiogenic antibody array

Angiogenic factors regulated by ELF3 were analyzed in SKOV3 cells using the ab193655-Human Angiogenesis Antibody Array Membrane (43 targets) (ab193655, Abcam). This experiment was carried out according to the protocol provided by the manufacturer. Briefly, SKOV3 cells were seeded in 100-mm culture dishes and incubated for 24 h. Cells were transfected with empty vector or human ELF3-inserted plasmid DNA. After 6 h, cells were replaced with a serum-free medium and then incubated for 20 h. Cells were lysed with the supplied 1× cell lysis buffer, and total protein concentration was determined using the BCA protein assay kit. Each membrane was treated with 500 µg of total protein in 1 ml of 1× blocking solution followed by incubation for 5 h at RT. After washing with the buffer, the membranes were incubated overnight with 1× Biotinylated Antibody Cocktail. Following washing, the membranes were added with 1× HRP-Conjugated Streptavidin and incubated for 2 h at RT. The results were confirmed by LAS-3000 (Fuji Photo Film Co. Ltd., Japan) using the provided detection buffer.

Clinical database analysis

To find genes that are highly expressed in hypoxia compared with normoxia, we used GENE-E software (version 3.0.215) to generate a heat map using GSE55564 (Koizume *et al*, 2015). To confirm the expression levels of the predicted 51 TFs, they were compared with three clinical datasets provided by the cBio Cancer Genomics portal (cBioPortal v3.7.25; <https://www.cbioportal.org/>): ovarian serous cystadenocarcinoma (TCGA, PanCanAtlas, *n* = 585), breast invasive carcinoma (TCGA, PanCanAtlas, *n* = 1082), prostate adenocarcinoma (TCGA, PanCanAtlas, *n* = 489), and lung adenocarcinoma (TCGA, PanCanAtlas, *n* = 507). Differences in the expression of 51 TFs between the normal ovary and EOC were identified using GSE36668 (Elgaaen *et al*, 2012). To investigate the relationship between ELF3 and IGF1, a clinical dataset from OC patients (TCGA, PanCanAtlas, *n* = 585) was used. GSE36668 was used to identify differences in the gene expression of 51 TFs between the normal ovary, serous ovarian borderline tumor, and serous ovarian carcinoma.

Statistical analysis

The number of repetitions for each experiment is indicated in the figure legends for each assay where all data were expressed as mean value ± standard deviation (mean ± SD). Statistical analysis was

performed using GraphPad Prism (Version 6.01, GraphPad Software, USA). The significance of the difference between the two groups was determined using a two-tailed and unpaired *t*-test of students. When the values were nominalized, the data without variance was subjected to a nonparametric statistical analysis. Differences between three or more independent groups were analyzed using one-way ANOVA or two-way ANOVA followed by the Tukey, Holm Sidak, or Sidak's multiple comparison test or Kruskal–Wallis followed by the Dunn's multiple comparison test. A $P < 0.05$ was considered statistically significant.

Data availability

This study includes no data deposited in external repositories.

Expanded View for this article is available online.

Acknowledgments

This work was supported by the Health Fellowship Foundation and the National Research Foundation of Korea (NRF) grant funded by the Korean government (MSIT) (2018R1A5A2025286) and by the Bio & Medical Technology Development Program of the NRF funded by MSIT (2021M3E5E7024855).

Author contributions

Seung Hee Seo: Conceptualization; Formal analysis; Investigation; Methodology; Writing—original draft; Project administration; Writing—review and editing. **Soo-Yeon Hwang:** Investigation; Writing—review and editing. **Seohui Hwang:** Investigation. **Sunjung Han:** Investigation. **Hyojin Park:** Investigation. **Yun-Sil Lee:** Writing—review and editing. **Seung Bae Rho:** Writing—review and editing. **Youngjoo Kwon:** Funding acquisition; Validation; Project administration; Writing—review and editing.

In addition to the CRediT author contributions listed above, the contributions in detail are:

SHS, Y-SL, SBR, and YK conceived the study. SHS and YK coordinated the project and wrote the manuscript. SHS performed most of the experiments. SHS and SHW conducted animal experiments. SHS, SHa, and HP performed experiments to confirm changes in the mRNA levels of proangiogenic factors regulated by ELF3. SHS and S-YH quantitatively analyzed the *in vitro* and *ex vivo* experimental results. All authors have read and agreed to the published version of the manuscript.

Disclosure and competing interests statement

The authors declare that they have no conflict of interest.

References

- Andrysiak Z, Bender H, Galbraith MD, Espinosa JM (2021) Multi-omics analysis reveals contextual tumor suppressive and oncogenic gene modules within the acute hypoxic response. *Nat Commun* 12: 1375
- Bach LA (2015) Endothelial cells and the IGF system. *J Mol Endocrinol* 54: R1–R13
- Baker M, Robinson SD, Lechertier T, Barber PR, Tavora B, D'Amico G, Jones DT, Vojnovic B, Hodivala-Dilke K (2011) Use of the mouse aortic ring assay to study angiogenesis. *Nat Protoc* 7: 89–104
- Bergers G, Benjamin LE (2003) Tumorigenesis and the angiogenic switch. *Nat Rev Cancer* 3: 401–410
- Boes M, Dake BL, Bar RS (1991) Interactions of cultured endothelial cells with TGF-beta, bFGF, PDGF and IGF-I. *Life Sci* 48: 811–821
- Brown C, Gaspar J, Pettit A, Lee R, Gu X, Wang H, Manning C, Voland C, Goldring SR, Goldring MB et al (2004) ESE-1 is a novel transcriptional mediator of angiopoietin-1 expression in the setting of inflammation. *J Biol Chem* 279: 12794–12803
- Burger RA, Brady MF, Bookman MA, Monk BJ, Walker JL, Homesley HD, Fowler J, Greer BE, Boente M, Fleming GF et al (2014) Risk factors for GI adverse events in a phase III randomized trial of bevacizumab in first-line therapy of advanced ovarian cancer: a Gynecologic Oncology Group Study. *J Clin Oncol* 32: 1210–1217
- Cannistra SA (2004) Cancer of the ovary. *N Engl J Med* 351: 2519–2529
- Chen H, Chen W, Zhang X, Hu L, Tang G, Kong J, Wang Z (2019) E26 transformation (ETS)specific related transcription factor3 (ELF3) orchestrates a positive feedback loop that constitutively activates the MAPK/Erk pathway to drive thyroid cancer. *Oncol Rep* 41: 570–578
- Chen J, Fu YI, Day DS, Sun YE, Wang S, Liang X, Gu F, Zhang F, Stevens SM, Zhou P et al (2017) VEGF amplifies transcription through ETS1 acetylation to enable angiogenesis. *Nat Commun* 8: 383
- Chen Z, Han ZC (2008) STAT3: a critical transcription activator in angiogenesis. *Med Res Rev* 28: 185–200
- Chung AS, Lee J, Ferrara N (2010) Targeting the tumour vasculature: insights from physiological angiogenesis. *Nat Rev Cancer* 10: 505–514
- Coleman RL, Monk BJ, Sood AK, Herzog TJ (2013) Latest research and treatment of advanced-stage epithelial ovarian cancer. *Nat Rev Clin Oncol* 10: 211–224
- Cross MJ, Claesson-Welsh L (2001) FGF and VEGF function in angiogenesis: signalling pathways, biological responses and therapeutic inhibition. *Trends Pharmacol Sci* 22: 201–207
- Dey N, De P, Brian LJ (2015) Evading anti-angiogenic therapy: resistance to anti-angiogenic therapy in solid tumors. *Am J Transl Res* 7: 1675–1698
- Ding M, Bruick RK, Yu Y (2016) Secreted IGFBP5 mediates mTORC1-dependent feedback inhibition of IGF-1 signalling. *Nat Cell Biol* 18: 319–327
- Eckel KL, Tentler JJ, Cappetta GJ, Diamond SE, Gutierrez-Hartmann A (2003) The epithelial-specific ETS transcription factor ESX/ESE-1/Elf-3 modulates breast cancer-associated gene expression. *DNA Cell Biol* 22: 79–94
- Elgaaen BV, Olstad OK, Sandvik L, Odegaard E, Sauer T, Staff AC, Gautvik KM (2012) ZNF385B and VEGFA are strongly differentially expressed in serous ovarian carcinomas and correlate with survival. *PLoS One* 7: e46317
- Eliceiri BP, Paul R, Schwartzberg PL, Hood JD, Leng J, Cheresch DA (1999) Selective requirement for Src kinases during VEGF-induced angiogenesis and vascular permeability. *Mol Cell* 4: 915–924
- Fukuda R, Hirota K, Fan F, Jung YD, Ellis LM, Semenza GL (2002) Insulin-like growth factor 1 induces hypoxia-inducible factor 1-mediated vascular endothelial growth factor expression, which is dependent on MAP kinase and phosphatidylinositol 3-kinase signaling in colon cancer cells. *J Biol Chem* 277: 38205–38211
- Gerber HP, McMurtrey A, Kowalski J, Yan M, Keyt BA, Dixit V, Ferrara N (1998) Vascular endothelial growth factor regulates endothelial cell survival through the phosphatidylinositol 3'-kinase/Akt signal transduction pathway. Requirement for Flk-1/KDR activation. *J Biol Chem* 273: 30336–30343
- Gondkar K, Patel K, Krishnappa S, Patil A, Nair B, Sundaram GM, Zea TT, Kumar P (2019) E74 like ETS transcription factor 3 (ELF3) is a negative

- regulator of epithelial- mesenchymal transition in bladder carcinoma. *Cancer Biomark* 25: 223–232
- Graybill W, Sood AK, Monk BJ, Coleman RL (2015) State of the science: emerging therapeutic strategies for targeting angiogenesis in ovarian cancer. *Gynecol Oncol* 138: 223–226
- Heo SH, Cho JY (2014) ELK3 suppresses angiogenesis by inhibiting the transcriptional activity of ETS-1 on MT1-MMP. *Int J Biol Sci* 10: 438–447
- Hofmann M, Heineke J (2019) The impact of endothelial transcription factors in sprouting angiogenesis. In *Tumor Angiogenesis*, Marmé D (ed), pp. 73–90. Cham: Springer, Cham
- Jeong HW, Hernandez-Rodriguez B, Kim J, Kim KP, Enriquez-Gasca R, Yoon J, Adams S, Scholer HR, Vaquerizas JM, Adams RH (2017) Transcriptional regulation of endothelial cell behavior during sprouting angiogenesis. *Nat Commun* 8: 726
- Kapoor A, Chen CG, Iozzo RV (2020) A simplified aortic ring assay: A useful ex vivo method to assess biochemical and functional parameters of angiogenesis. *Matrix Biol Plus* 6–7: 100025
- Kar A, Gutierrez-Hartmann A (2017) ESE-1/ELF3 mRNA expression associates with poor survival outcomes in HER2(+) breast cancer patients and is critical for tumorigenesis in HER2(+) breast cancer cells. *Oncotarget* 8: 69622–69640
- Kar A, Liu B, Gutierrez-Hartmann A (2017) ESE-1 knockdown attenuates growth in Trastuzumab-resistant HER2(+) breast cancer cells. *Anticancer Res* 37: 6583–6591
- Kerbel R, Folkman J (2002) Clinical translation of angiogenesis inhibitors. *Nat Rev Cancer* 2: 727–739
- Koizume S, Ito S, Nakamura Y, Yoshihara M, Furuya M, Yamada R, Miyagi E, Hirahara F, Takano Y, Miyagi Y (2015) Lipid starvation and hypoxia synergistically activate ICAM1 and multiple genes in an Sp1-dependent manner to promote the growth of ovarian cancer. *Mol Cancer* 14: 77
- Kuang L, Li L (2021) E74-like factor 3 suppresses microRNA-485-5p transcription to trigger growth and metastasis of ovarian cancer cells with the involvement of CLDN4/Wnt/beta-catenin axis. *Saudi J Biol Sci* 28: 4137–4146
- Li D, Cheng P, Wang J, Qiu X, Zhang X, Xu L, Liu Y, Qin S (2019) IRF6 is directly regulated by ZEB1 and ELF3, and predicts a favorable prognosis in gastric cancer. *Front Oncol* 9: 220
- Lin S, Zhang Q, Shao X, Zhang T, Xue C, Shi S, Zhao D, Lin Y (2017) IGF-1 promotes angiogenesis in endothelial cells/adipose-derived stem cells co-culture system with activation of PI 3K/Akt signal pathway. *Cell Prolif* 50: e12390
- Liu Y, Wang S, Zhou R, Li W, Zhang G (2021) Overexpression of E74-like transformation-specific transcription factor 3 promotes cellular proliferation and predicts poor prognosis in ovarian cancer. *Oncol Lett* 22: 710
- Longoni N, Sarti M, Albino D, Civenni G, Malek A, Ortelli E, Pinton S, Mello-Grand M, Ostano P, D'Ambrosio G et al (2013) ETS transcription factor ESE1/ELF3 orchestrates a positive feedback loop that constitutively activates NF- κ B and drives prostate cancer progression. *Can Res* 73: 4533–4547
- Lung HL, Lung ML (2012) *In vivo* matrigel plug angiogenesis assay. *Bio-protocol* 2: e261
- Meadows SM, Myers CT, Krieg PA (2011) Regulation of endothelial cell development by ETS transcription factors. *Semin Cell Dev Biol* 22: 976–984
- Ouni M, Belot MP, Castell AL, Fradin D, Bougneres P (2016) The P2 promoter of the IGF1 gene is a major epigenetic locus for GH responsiveness. *Pharmacogenomics J* 16: 102–106
- Potente M, Gerhardt H, Carmeliet P (2011) Basic and therapeutic aspects of angiogenesis. *Cell* 146: 873–887
- Ribatti D, Ranieri G, Basile A, Azzariti A, Paradiso A, Vacca A (2012) Tumor endothelial markers as a target in cancer. *Expert Opin Ther Targets* 16: 1215–1225
- Robinson RS, Woad KJ, Hammond AJ, Laird M, Hunter MG, Mann GE (2009) Angiogenesis and vascular function in the ovary. *Reproduction* 138: 869–881
- Spannuth WA, Sood AK, Coleman RL (2008) Angiogenesis as a strategic target for ovarian cancer therapy. *Nat Clin Pract Oncol* 5: 194–204
- Stoeltzing O, Liu W, Reinmuth N, Fan F, Parikh AA, Bucana CD, Evans DB, Semenza GL, Ellis LM (2003) Regulation of hypoxia-inducible factor-1 α , vascular endothelial growth factor, and angiogenesis by an insulin-like growth factor-I receptor autocrine loop in human pancreatic cancer. *Am J Pathol* 163: 1001–1011
- Takahashi T, Ueno H, Shibuya M (1999) VEGF activates protein kinase C-dependent, but Ras-independent Raf-MEK-MAP kinase pathway for DNA synthesis in primary endothelial cells. *Oncogene* 18: 2221–2230
- Teleanu RI, Chircov C, Grumezescu AM, Teleanu DM (2019) Tumor angiogenesis and anti-angiogenic strategies for cancer treatment. *J Clin Med* 9: 84
- Teng JA, Wu SG, Chen JX, Li Q, Peng F, Zhu Z, Qin J, He ZY (2016) The activation of ERK1/2 and JNK MAPK Signaling by insulin/IGF-1 is responsible for the development of colon cancer with type 2 diabetes mellitus. *PLoS One* 11: e0149822
- Treins C, Giorgetti-Peraldi S, Murdaca J, Semenza GL, Van Obberghen E (2002) Insulin stimulates hypoxia-inducible factor 1 through a phosphatidylinositol 3-kinase/target of rapamycin-dependent signaling pathway. *J Biol Chem* 277: 27975–27981
- Walker DM, Poczobutt JM, Gonzales MS, Horita H, Gutierrez-Hartmann A (2010) ESE-1 is required to maintain the transformed phenotype of MCF-7 and ZR-75-1 human breast cancer cells. *Open Cancer J* 3: 77–88
- Walsh LA, Damjanovski S (2011) IGF-1 increases invasive potential of MCF 7 breast cancer cells and induces activation of latent TGF- β 1 resulting in epithelial to mesenchymal transition. *Cell Commun Signal* 9: 10
- Wang H, Xu T, Zheng L, Li G (2018a) Angiogenesis inhibitors for the treatment of ovarian cancer: an updated systematic review and meta-analysis of randomized controlled trials. *Int J Gynecol Cancer* 28: 903–914
- Wang H, Yu Z, Huo S, Chen Z, Ou Z, Mai J, Ding S, Zhang J (2018b) Overexpression of ELF3 facilitates cell growth and metastasis through PI3K/Akt and ERK signaling pathways in non-small cell lung cancer. *Int J Biochem Cell Biol* 94: 98–106
- Wang JL, Chen ZF, Chen HM, Wang MY, Kong X, Wang YC, Sun TT, Hong J, Zou W, Xu J et al (2014) Elf3 drives beta-catenin transactivation and associates with poor prognosis in colorectal cancer. *Cell Death Dis* 5: e1263
- Xu H, Wang H, Li G, Jin X, Chen B (2021) The immune-related gene ELF3 is a novel biomarker for the prognosis of ovarian cancer. *Int J Gen Med* 14: 5537–5548
- Yadav L, Puri N, Rastogi V, Satpute P, Sharma V (2015) Tumour angiogenesis and angiogenic inhibitors. A Review. *J Clin Diagn Res* 9: XE01–XE05
- Zhang Y, Wang X, Chen X (2021) Identification of core genes for early diagnosis and the EMT modulation of ovarian serous cancer by bioinformatics perspective. *Aging* 13: 3112–3145
- Zhang Z, Zhang J, Li J, Geng H, Zhou B, Zhang B, Chen H (2020) miR-320/ELF3 axis inhibits the progression of breast cancer via the PI3K/AKT pathway. *Oncol Lett* 19: 3239–3248

- Zhao W, Sun Q, Yu Z, Mao S, Jin Y, Li J, Jiang Z, Zhang Y, Chen M, Chen P et al (2018) MiR-320a-3p/ELF3 axis regulates cell metastasis and invasion in non-small cell lung cancer via PI3K/Akt pathway. *Gene* 670: 31–37
- Zheng L, Xu M, Xu J, Wu KE, Fang Q, Liang Y, Zhou S, Cen D, Ji L, Han W et al (2018) ELF3 promotes epithelial-mesenchymal transition by protecting ZEB1 from miR-141-3p-mediated silencing in hepatocellular carcinoma. *Cell Death Dis* 9: 387



License: This is an open access article under the terms of the Creative Commons Attribution-NonCommercial-NoDerivs 4.0 License, which permits use and distribution in any medium, provided the original work is properly cited, the use is non-commercial and no modifications or adaptations are made.